Carbohydrate Polymers 83 (2011) 979–987

Contents lists available at ScienceDirect

Carbohydrate Polymers

journal homepage: www.elsevier.com/locate/carbpol

Nano-biomaterials application: *In situ* modification of bacterial cellulose structure by adding HPMC during fermentation

Huang-Chan Huang[a], Li-Chen Chen[a,*], Shih-Bin Lin[a,b,**], Hui-Huang Chen[a,b,***]

[a] *Institute of Biotechnology, National Ilan University, Ilan 26047, Taiwan*
[b] *Department of Food Science, National Ilan University, Ilan 26047, Taiwan*

ARTICLE INFO

Article history:
Received 13 February 2010
Received in revised form 2 September 2010
Accepted 6 September 2010
Available online 15 September 2010

Keywords:
Bacterial cellulose
HPMC
In situ fermentation
Rehydration
Crystallinity

ABSTRACT

Bacterial cellulose (BC) has been studied as biomedical material due to its nanoscale fiber network, biocompatibility, and high water holding capacity. However, BC exhibits a poor rehydration after drying due to its high crystallinity. In this study, hydroxypropylmethyl cellulose (HPMC) was added into a BC fermentation culture medium to interfere with the formation of BC structure *in situ* and create a modified BC, named HBC. Notably, mechanical strength in HBC declined. SEM images showed that, while the cellulose bundle width of HBC was enlarged, the cellulose network void in HBC shrank. X-ray diffraction and FTIR analysis revealed that the addition of HPMC reduced the crystallinity index (*CrI*). HBC also exhibited the highest rehydration ratio as well as the lowest crystallinity at 0.75% HPMC addition level (named 0.75%HBC). The 0.75%HBC also exhibited a higher composition ratio of EMG/BC composite and showed the improvement in water and small molecule absorption.

1. Introduction

Cellulose forms the basic structural foundation of cell walls in eukaryotic plants and algae and is also a major constituent of cell walls in fungi (Cannon & Anderson, 1991). It is therefore, the most abundant bio-polymer on the planet with 180 billion tons per year produced in nature (Engelhardt, 1995). Bacteria also synthesize cellulose, including the genera *Acetobacter*, *Agrobacteria*, *Rhizobia*, *Sarcina*, *Pseudomonas*, *Achromobacter*, *Alcaligenes*, *Aerobacter*, and *Azotobacter* (Jonas & Farah, 1998). *Acetobacter xylinum*, a Gram-negative, rod shaped bacteria and a prodigious producer of cellulose, has been studied extensively and renamed *Gluconacetobacter xylinus* subsp. *xylinus* in 1997 (Yamada, Hoshino, & Ishikawa, 1997, 1998).

Bacterial cellulose (BC) is composed of nano-sized fibers where the nanofiber structuring determines the product properties (Klemm et al., 2006). Materials based on this type of cellulose have become increasingly important and are part of an innovative pool for bio-material development. As such, bacterial synthesized cellulose is of special interest because of its unique specific structure and properties. This BC is quite different from plant cellulose and takes centre stage in our investigations. It is defined by high purity (free of hemicellulose, lignin, and alien functionalities such as carbonyl or carboxyl groups) and a high degree of polymerization (up to 8000). Moreover, it is specifically characterized by its high crystallinity (80–90%) and a water-swollen nanofiber network (99% water) (Zugenmaier, 2001). BC is shaped during cultivation and examples are given in different thickness layers, thin foils, and various types of tubes. Contrary to plant cellulose, BC can be used directly in its biogenously formed molecular, supramolecular, and morphological structure without damage to the nanofiber network and the corresponding pore system (Kramer et al., 2006).

Microdiffraction investigation of nascent BC microfibrils showed that the reducing ends of the growing cellulose chains point away from the bacterium which provide direct evidence that polymerization by the cellulose synthase takes place at the non-reducing end of the growing cellulose chains (Koyama, Helbert, Imai, Sugiyama, & Henrissat, 1997). The crystallization of cellulose is induced during the aggregation processes because the sub-elementary fibrils may be too fine to crystallize. As parallel orientation of cellulose chains is already realized in each sub-elementary fibril, a somewhat local-level rearrangement of the chains should be enough to induce crystallization by aggregation of

* Corresponding author at: Department of Food Science, National Ilan University, No. 1, Sec. 1, Shen-Lung Rd., Ilan City, Ilan County 26047, Taiwan.
** Corresponding author at: Institute of Biotechnology, National Ilan University, No. 1, Sec. 1, Shen-Lung Rd., Ilan City, Ilan County 26047, Taiwan.
*** Corresponding author at: Department of Food Science, National Ilan University, No. 1, Sec. 1, Shen-Lung Rd., Ilan City, Ilan County 26047, Taiwan.
Tel.: +1 886 3 935 7400; fax: +1 886 3 935 1829.
E-mail addresses: upup623@yahoo.com.tw (H.-C. Huang), ywchen@niu.edu.tw (L.-C. Chen), sblin@niu.edu.tw (S.-B. Lin), hhchen@niu.edu.tw (H.-H. Chen).

0144-8617/$ – see front matter © 2010 Elsevier Ltd. All rights reserved.
doi:10.1016/j.carbpol.2010.09.011

sub-elementary fibrils into a microfibril through hydrogen bonding (Hirai, Tsuji, Yamamoto, & Horii, 1998).

Furthermore, the addition of some polymers can drastically modify the cellulose biosynthesis. The addition of carboxymethylcellulose (CMC) into the culture medium alters the crystallization and assembly of the cellulose fibrils (Haigler, White, Brown, & Cooper, 1982). Grande, Torres, Gomez, and Bano (2009) had prepared BC-hydroxyapatite (HAp) nanocomposites by introducing CMC into the bacteria culture media. Moreover, the biocompatibility of the materials and the bioactivity of HAp are factors that make this nanocomposite a material with potential biomedical applications. However, few investigations have been made into the structural changes of bacterial cellulose membranes during the drying process and resultant physical and mechanical properties (Clasen, Sultanova, Wilhelms, Heisig, & Kulicke, 2006).

The hydrolyzed gelatin, enzymatically modified gelatin (EMG) in this study, exhibits unique functional properties whereby it has proven itself useful in the food industry (Intarasirisawata et al., 2007). Shimada, Yamamoto, and Sase (1984) and Yamamoto, Kusuhara, and Matsumoto (1984) found that papain hydrolyzed gelatin modified with leucine hexyl ester or leucine dodecyl ester could be used to fabricate hydrophilic surfactants. Lin, Hsu, Chen, and Chen (2009) also found that, when BC was immersed in an EMG solution, the EMG penetrated BC networks and formed a composite, improving the rehydration ability of dried BC. Nevertheless, the penetration speed was slow and the EMG content of the composite was limited to around 50%.

Therefore, the objectives of this study were to introduce hydroxypropylmethyl cellulose (HPMC) during fermentation to interfere with *in situ* BC crystallization by preventing the gathering of myofibrils or cellulose ribbons. Improvements in the rehydration properties and low molecular compounds, hydrophilic EMG, absorption ability of the resultant structurally modified BC were expected.

2. Materials and methods

2.1. BC preparation

G. xylinum (BCRC12335), purchased from FIRDI (Food Industry Research and Development Institute, Hsinchu, Taiwan), was cultured with a 500 mL mannitol broth medium containing 25 g/L mannitol, 5 g/L yeast extract and 3 g/L peptone in a 1 L flask shaken for 24 h at 30 °C. *G. xylinum* was enumerated using a spreading plate technique with a mannitol agar medium. Modified coconut juice media, containing 0.2% acetic acid and 10° Brix soluble solid content adjusted with sucrose, was inoculated with *G. xylinum* culture (10%, v/v) and cultivated statically at 30 °C in 250 mL flasks for 14 days. HPMC (300 mPa s for 2% gel solution at 20 °C and the substitution of methoxyl and hydroxy-propoxyl are 23% and 10%, respectively), purchased from Toong Yeuan Enterprise Co. Ltd. (Taipei, Taiwan), was then introduced into *in situ* fermentation with a concentrations range from 0 to 1.0%. The HPMC created modified BC (MBC) fermentation, identified as HBC. To eliminate impurities such as bacteria and other interfering substances, cellulose cake floating on the culture was collected and boiled in 0.5N NaOH for 10 min, followed by immersion in 0.5N NaOH for 24 h at room temperature followed by deionized water rinse to achieve a neutral pH (Hong et al., 2006).

2.2. EMG preparation

The fish gelatin purchased from Jellice Pioneer Private Ltd. (Pingtung, Taiwan), was prepared from tilapia skin and had a bloom value of 203 g. Gelatin was hydrolyzed with 1% Alcalase (pH 6.5) at 50 °C and was terminated at 20 min by boiling for 15 min.

2.3. EMG/BC composites preparation and composition ratio

In accordance to the methodology of Nakayama et al. (2004), alkali treated BC was immersed in 0.5% EMG solution (w/v = 1/10) at 50 °C for 1 week in order to become a composite.

Hydroxyproline content was analyzed using the methods of Reddy and Enwemeka (1996). The freeze-dried sample was dissolved with 2.0N NaOH to prepare 1% solution and homogenized (Silverson L4R, Silverson Machines Ltd., Buckinghamshire, England) for 1 min, and heated in a water bath at 60 °C for 30 min and centrifuged. 0.2 mL supernatant was mixed with 0.3 mL 3.3N NaOH and hydrolyzed at 120 °C for 60 min. The hydrolysate was mixed with 4.5 mL Chloramine-T reagent and an acetate/citrate buffer (1.27 g Chloramine-T was dissolved in 20 mL 50% n-propanol, added to an acetate-citrate buffer (pH 6.5) to 100 mL) and oxidized at 25 °C for 25 min. 5 mL Ehrlich's reagent solution (15 g p-dimethylaminobenzaldehyde was dissolved in propanol/prechloic acid at a ratio of 2:1 (v/v) to 100 mL) was added and mixed thoroughly and then heated in a water bath at 60 °C for 20 min to produce Chromophores. Absorbance was measured at 550 nm. EMG content in the dried composite was calculated as:

$$\text{EMG content}\,(\%) = [\text{Sample Hyp}\,(\text{mg/mL}) \times 5000 \times 11.34 \times 10^{-4}]$$

where Hyp represents hydroxyproline. The conversion factor for calculating the gelatin content from the hydroxyproline of the sample was 11.34 and dilution factor was 5000. There was a 10^{-4} factor for μg/mL to % when the density of the solution is hypothetical to 1 g/mL (Muyonga, Cole, & Duodu, 2004). The composition ratio of the composite was calculated as:

$$\text{composition ratio} = \frac{\text{EMG content}}{\text{BC content}}$$

2.4. Rheological properties

The rheological properties of BC and HBC were determined with a dynamic rheometer (Rheometer AR-550, TA Instruments, New Castle, Delaware, USA) using a small amplitude oscillatory test (SAOT). The dynamic rheometer was equipped with rough surface parallel-plate geometry (20 mm diameter with 1 mm deep crisscross grooves) to prevent sample slippage. Gap and strain were set at 2.0 mm and 1.0%, respectively. The frequency sweeps were conducted between 0.01 and 10 Hz at 20 °C. Three replicate scans were conducted, with storage modulus (G'), loss modulus (G''), tan δ and complex viscosity magnitude (η^*) recorded.

2.5. SEM observation

BC and HBC were ruptured into small pieces after freeze-drying. Dried specimens were mounted on aluminum studs and coated with a gold/palladium alloy under high vacuum conditions. Specimens were examined using a Tescan Vega TS5136MM microscope (Tescan s.r.o., Brno, Czech Republic) to observe the microstructure of ruptured surfaces.

2.6. X-ray diffraction

The crystallinities of HPMC, BC, and HBC were determined by an X-ray diffractometer (X'Pert PRO, PANalytical, Netherlands) using Ni-filtered CuK radiation (λ = 1.54 Å). Operating voltage and current were 40 kV and 30 mA, respectively. Degree of crystallinity (Crystallinity index, *CrI*) was calculated from diffracted intensity data using a method described by Segal, Creely, Martin, and Conrad

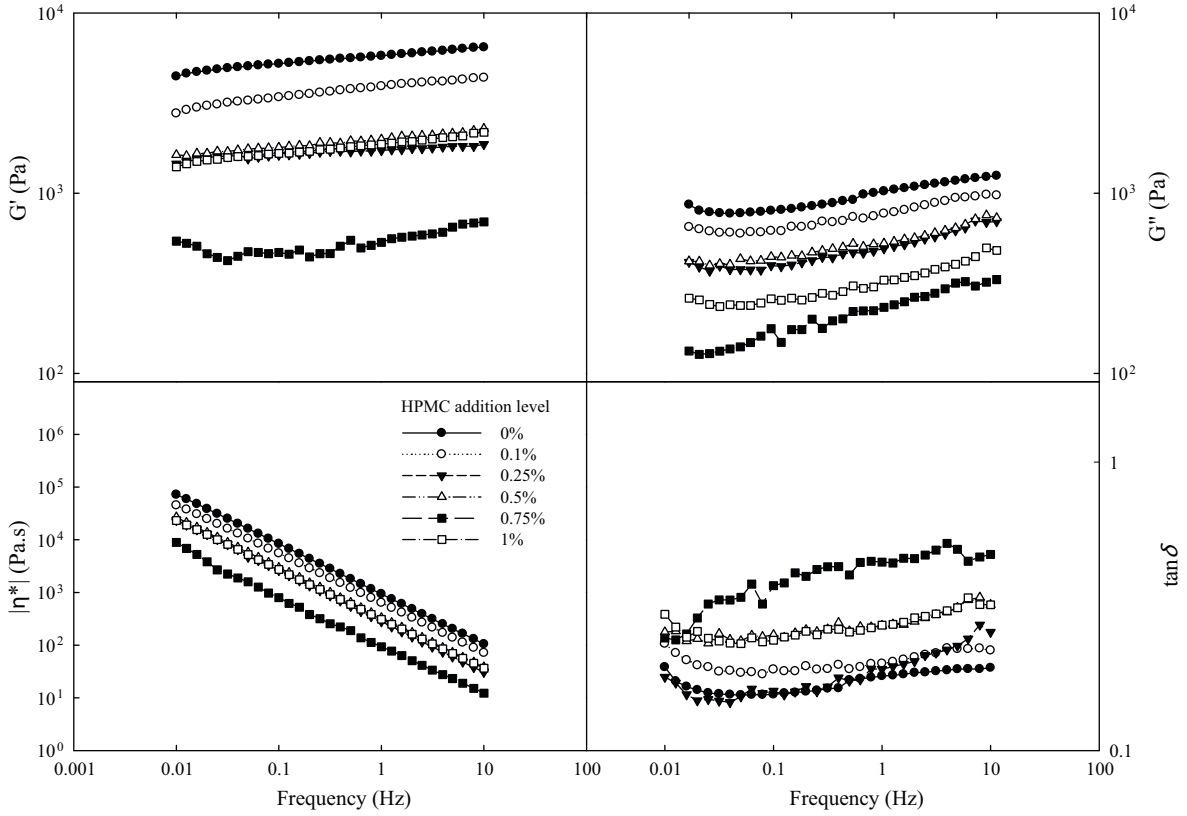

Fig. 1. Rheological property of HBC prepared by *in situ* fermentation with different addition levels of HPMC.

(1959):

$$CrI(\%) = \left(1 - \left(\frac{I_{AM}}{I_{200}}\right)\right) \times 100\%$$

The I_{AM} and I_{200} represent intensity of diffraction in the same units at approximately $2\theta = 18^\circ$ and maximum intensity of the (0 0 2) lattice diffraction at approximately $2\theta = 22.7^\circ$, respectively.

2.7. Fourier Transform Infrared (FT-IR) Spectroscopy

FT-IR spectra of freeze-dried BC and HBC were recorded on a Paragon 500 (PerkinElmer, Waltham, USA) in absorption mode in the range of 4000–450 cm^{-1}. Thirty-two scans were performed to establish accuracy.

2.8. Water holding capacity (WHC) and rehydration ratio

Following Embuscado, BeMiller, and Marks (1996) and Okiyama, Motoki, and Yamanaka (1992), wet BC and HBC were drained at 25 °C for 2 min and weighed (Wwet). The material was then centrifuged at 8000 × *g* for 30 min, after which the supernatant was weighed (Wsup). Sediment was then freeze-dried and weighed (Wdry). Water holding capacities of BC and HBC were calculated as:

$$\text{WHC}(\%) = \frac{(\text{Wwet} - \text{Wdry}) - \text{Wsup}}{\text{Wdry}} \times 100\%$$

In accordance with the methodology proposed by Bodhibukkana et al. (2006), freeze-dried BC and composite materials (with 100 mm length, 30 mm width and 2 mm thickness) were weighed (Wdry) and immersed in deionized water (w/v = 1:2) until the weight of the rehydrated sample (Wrwet) no longer increased (around 7 h). The rehydration ratio, representing the degree to which removed water was replaced by water, was calculated as:

$$\text{rehydration ratio}(\%) = \frac{\text{Wrwet} - \text{Wdry}}{\text{Wwet} - \text{Wdry}} \times 100\%$$

2.9. Statistical analysis

Statistical analysis of data was performed using an SPSS system. When analysis of variance (ANOVA) revealed a significant effect ($p < 0.05$), data means were compared using a least significant difference (LSD) test.

3. Results and discussion

3.1. Rheological properties

The rheological moduli and η^* of HBC exhibited similar tendencies during frequency sweeps (Fig. 1). The addition of HPMC to the media caused the lowering of moduli and η^* of HBC. However, the HBC prepared with the 0.75% HPMC during *in situ* fermentation exhibited the lowest moduli and η^*, but the highest tan δ.

The rheological moduli may reflect inner structural developments and molecular interactions during network formation (Musampa, Alves, & Maia, 2007). Young's modulus of a BC sheet can be attributed mainly to the ultrafine structure of ribbons, which allows more extensive H-bonds to form in a cellulose mass (Nishi et al., 1990; Yamanaka et al., 1989). Therefore, fewer H-bonds formed during the assembly of cellulose ribbons is suggested to result in lower 0.75%HBC moduli.

An ideal gel has a G' value which is relatively independent of frequency over a broad range, while a hydrocolloid exhibits pseudo-gel properties under conditions in which its G' is frequency dependent (Morris & Ross-Murphy, 1981). Since G' shows a signif-

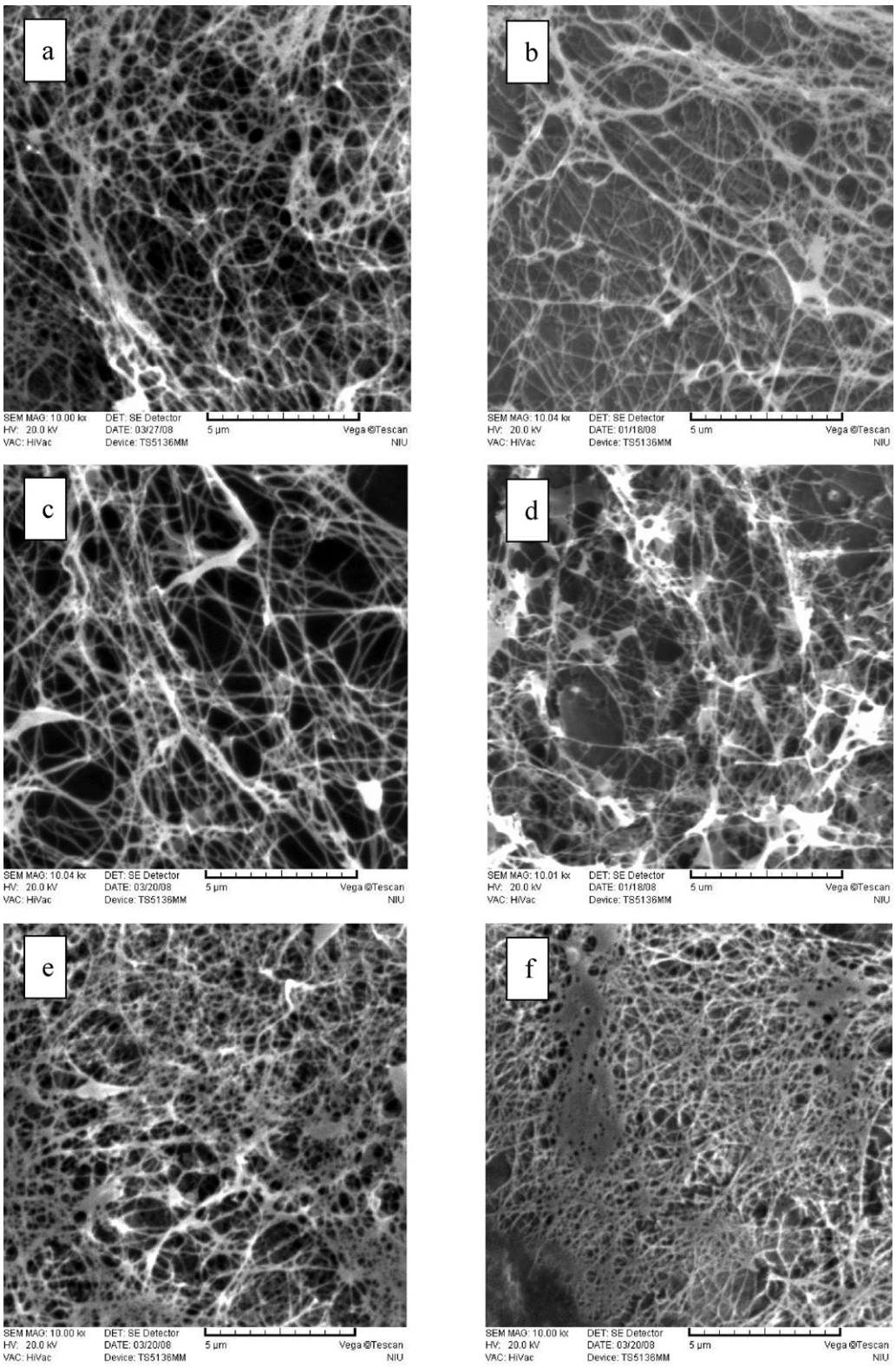

Fig. 2. SEM images of HBC prepared by *in situ* fermentation with different HPMC addition levels of 0% (a), 0.1% (b), 0.25% (c), 0.5% (d), 0.75% (e), and 1% (f).

icant frequency dependence (Fig. 1), BC suspension also behaves as a pseudo-gel. This is due to the excellent dispersion properties of statically grown BC, which has a water holding capacity of about 200 times its dry weight (Okiyama, Motoki, & Yamanaka, 1993). The fact that the participation of HPMC did not enhance HBC moduli indicated that their colloid does not exhibit tough networks.

3.2. Micro-structure

A cellulose network consisting of nanoscale cellulose was observed in BC (Fig. 2a). The cellulose ribbon diameter was enlarged and voids between cellulose ribbons were shrunk in HBC (Fig. 2b–f), with cellulose networks being significantly different from those of

BC. The voids between cellulose ribbons were almost filled when 1% HPMC was added during *in situ* fermentation (Fig. 2f).

The BC ribbon assembly formed by *G. xylinum* can be altered through incubation with water soluble cellulose derivatives. Substituted celluloses prevent the normal fasciation of microfibril bundles which results in typical twisted-ribbon formations. Alteration of ribbon assemblies induced a synthesis of separate, intertwining bundles of microfibrils (Haigler et al., 1982; Hirai et al., 1998; Whitney, Brigham, Darke, Reid, & Gidley, 1995). HBC networks became more closely knit and the diameters of cellulose ribbons were enlarged. It has been suggested that the intertwining of HPMC with BC microfibrils alters the ribbon assembly, resulting in the formation of interpenetrating networks and voids diminution between cellulose ribbons.

Notably, HPMC was too large to enter the crystalline zone between subfibrils. Steric hindrance led HPMC to interfere mainly with the formation of H-bonds between microfibrils. Similar mechanisms behind interference by xylan and mannan in BC structures were reported by Yamamoto, Horii, and Hirai (1996) and Tokoh, Takabe, Sugiyama, and Fujita (2002). They concluded that, in a medium to which xylan or CMC had been added, only some of the additives influence cellulose microfibrils and inhibit aggregating (1 1 0) planes from forming ribbons (Haigler et al., 1982). Certain hydrocolloids such as HPMC are believe to associate randomly on the surface of individual microfibrils thus inhibiting aggregation of these microfibrils. These regions of reduced aggregation are located randomly along the cellulose bundles. The HPMC is draped over the cellulose microfibril surfaces and thus prevents more extensive aggregation or crystallization. Reduced aggregation may result in rehydration improvement.

3.3. X-ray diffraction and degree of crystallinity

Two main peaks, $2\theta = 22.7^\circ$ and 14.62°, were observed in the fitted diffractogram profiles of BC and HBC (Fig. 3). The position of $2\theta = 22.7^\circ$ and 14.62° peaks represent, respectively, the (0 0 2) and (1 1 0) lattice diffraction of cellulose (Segal et al., 1959). These peaks demonstrate that BC possesses cellulose I crystals (Oh et al., 2005; Uhlin, Atalla, & Thompson, 1995). On the other hand, HPMC dos not possess cellulose I crystals. The small variation in intensity accompanying angle changes and the low relative intensity of the (1 1 0) peak in HBC both suggest that the preferential orientation of the (1 1 0) plane to the reflection is disrupted by the addition of HPMC (Tokoh et al., 2002).

The ratio of peak intensities in X-ray diffractograms illustrates the degree of crystallite orientation. Decreases in the degree of crystallinity (*CrI*%) were observed in HBC (Table 1). Similar results were reported by Haigler et al. (1982). They concluded that the CMC adsorbed on fibrils and microfibrils was found to influence cellulose microfibrils aggregating (1 1 0) planes regarding the forming of ribbons, resulting in the hindrance of BC crystallization. Notably, HPMC is also a water soluble cellulose derivative with similar physical properties which suggests that the interfering mechanism of HPMC is analogous to that of CMC. Nevertheless, when 1% HPMC was added in fermentation, the residual HPMC which did not participate in the interference of BC microfibrils aggregating was then filled in the BC network. The thermal gelled HPMC oppressed cellulose bundles and forced the myofibrils to become closer during hot alkaline treatment. These phenomena facilitated the crystallization of HBC during drying. However, FTIR was employed to further evaluate the mechanism involved in impeding crystallization, which analyzed the effect of adding interfering substances on BC functional groups and bonds.

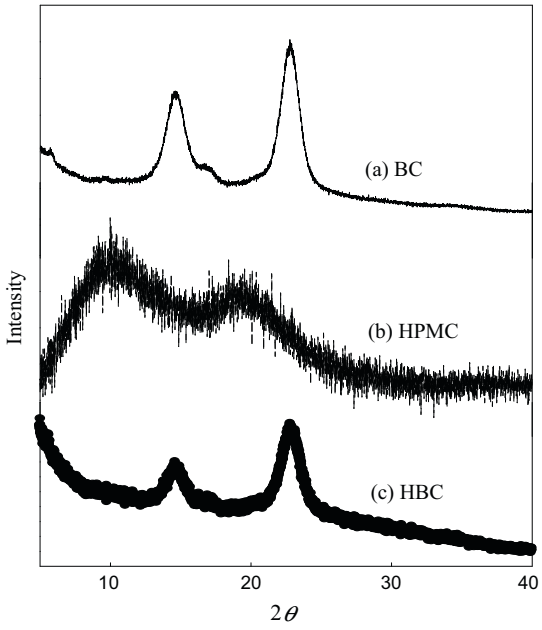

Fig. 3. X-ray diffraction patterns of cellulose.

3.4. FTIR analysis

The peak at 1641 cm^{-1} in spectrum (corresponding to C=O, or water in amorphous regions) (Fengel & Ludwig, 1991) of HPMC was bigger than that in BC. A distinctively small peak at 1427 cm^{-1} (corresponding to a crystal region of the cellulose) while a broader the peak in the region 3600–3200 cm^{-1} (corresponding to O–H cellulose stretching frequencies) (Maréchal & Chanzy, 2000) was observed in the HPMC (Fig. 4A). Compared to BC, the HPMC exhibited lower crystallization.

For HBC, the peaks in the region 3600–3200 cm^{-1} became noticeably broader as HPMC addition levels increased in the fermentation medium. A significant shoulder peak at 3240 cm^{-1} was evident in the BC spectrum while this peak shrunk or even disappeared in HBC (Fig. 4B). Furthermore, the peaks in the region 1034–1110 cm^{-1} shrunk or even disappeared while the peaks at 1634 cm^{-1} enlarged in HBC (Fig. 4C).

The peaks in the region 3600–3000 cm^{-1} correspond to O–H cellulose stretching frequencies (Maréchal & Chanzy, 2000). This is particularly useful in elucidating hydrogen-bonding patterns because, in favorable cases, each distinct hydroxyl group exhibits a single stretching band at a frequency that decreases with increasing hydrogen bonding strength (Šturcová, His, Apperley, Sugiyama, & Jarvis, 2004). In the cellulose crystals, the conformation of the cellulose chains and their strong packing depends on intermolecular

Table 1
Crystallinity index (*CrI*, %) of HPMC and HBC prepared by *in situ* fermentation with added interfering substances.

	HPMC	HPMC addition level in fermentation					
		0%	0.1%	0.25%	0.5%	0.75%	1%
CrI%	5.83 ± 1.98^{d}	70.54 ± 7.54^{a}	58.78 ± 5.51^{b}	46.84 ± 7.76^{bc}	44.52 ± 5.40^{c}	45.04 ± 3.25^{c}	52.23 ± 3.31^{b}

Values for each sample with different superscripts (a–d) are significantly different ($n = 3$, $p < 0.05$).

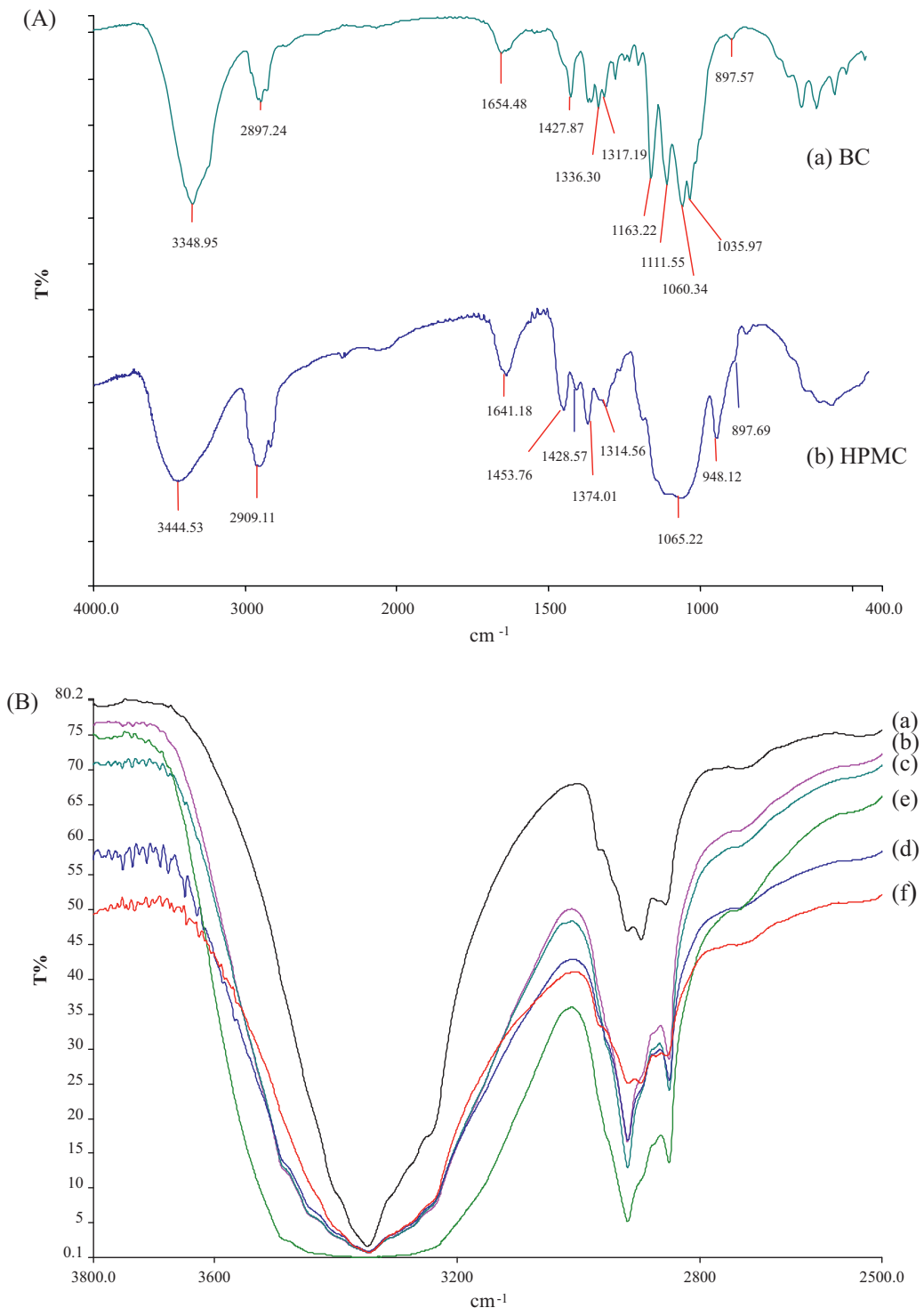

Fig. 4. (A) FTIR spectra of BC and HPMC; (B) FTIR spectra in 3600–2800 cm^{-1} of HBC prepared by *in situ* fermentation with different HPMC addition levels of 0% (a), 0.1% (b), 0.25% (c), 0.5% (d), 0.75% (e), and 1% (f); (C) FTIR spectra in 1700–850 cm^{-1} of MBC prepared by *in situ* fermentation with different HPMC addition levels of 0% (a), 0.1% (b), 0.25% (c), 0.5% (d), 0.75% (e), and 1% (f).

and intramolecular hydrogen bonds. The intramolecular hydrogen bonds for 2-OH···O-6 and 3-O···HO-5 and the intermolecular hydrogen bonds for 6-O···HO-3 in cellulose I appear at 3455–3410, 3375–3340 and 3310–3230 cm^{-1}, respectively, along with the valence vibration of H-bonded OH groups at 3570–3450 cm^{-1} (Oh et al., 2005). As the free-OH group peak appears at 3650–3590 cm^{-1} (Ivanova, Korolenko, Korolik, & Zbankov, 1989), the broader peak in the 3600–3200 cm^{-1} region of HBC implies that H-bonds in HBC were reduced.

Schwanninger, Rodrigues, Pereira, and Hinterstoisser (2004) found that the crystallinity of degraded cellulose decreased with ball milling. The peak around 3200 cm^{-1} became broader, which reflected the increase of free –OH caused by the ball milling damaging the H-bonds in cellulose. The diminishment in the spectra of

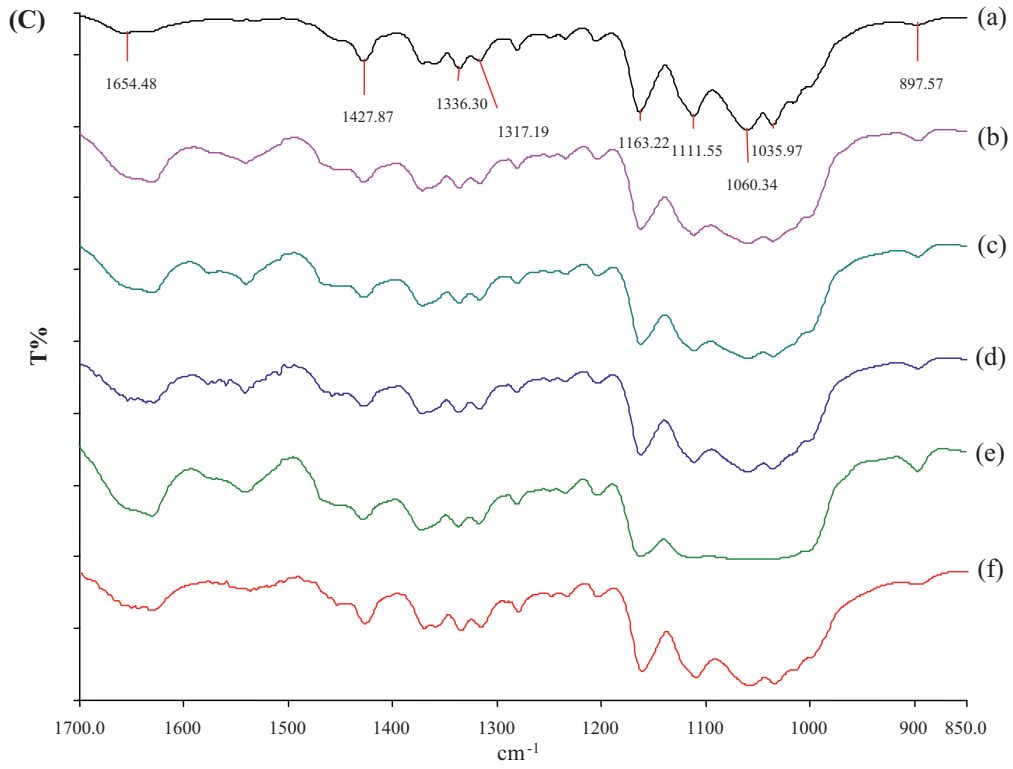

Fig. 4. (*Continued*).

milled cellulose was observed at wave numbers 1034, 1059, 1110, 1162, 1318, and 1335 cm^{-1}. These FT-IR spectra of crystallinity diminished cellulose were similar to those of HBC in this study.

The conspicuous changes in the peaks around 3400 cm^{-1} and in the fingerprint region were observed in 0.75%HBC. This phenomenon shows that the 0.75% addition level of HPMC in fermentation interferes with the formation of H-bonds between microfibrils.

3.5. HBC hydrophilic properties

The WHC of HBC declined as HPMC addition levels increased to 0.5% during fermentation (Fig. 5). The rehydration ratio of freeze-dried HBC increased as HPMC addition levels increased during fermentation. The maximum rehydration ratio, roughly twice as high as the control, was observed at 0.75% HBC regardless of the dried HBC being immersed for 10 min or 7 h (Fig. 6).

BC comprises a hydrophobic, ultrafine-fiber network stacked in a stratified structure that exhibits mechanical anisotropy with a high tensile modulus along the fiber-layer direction and a low compressive modulus perpendicular to the stratified direction. In an as-prepared BC containing more than 90% water, water is easily expelled with no further recovery in swelling properties due to the formation of H-bonds between cellulose fibers (Nakayama et al., 2004).

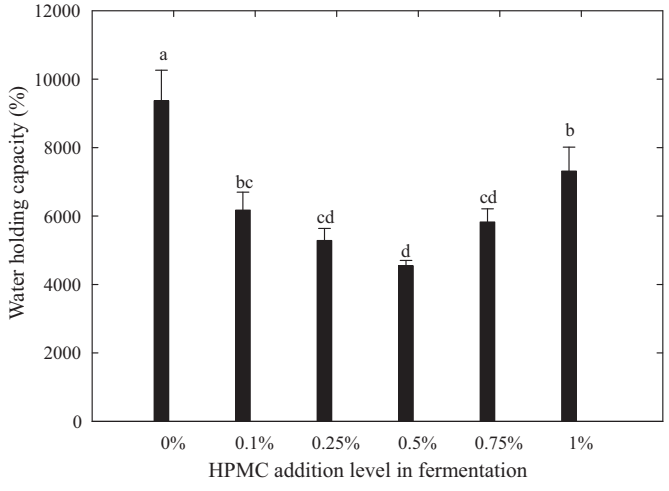

Fig. 5. Water holding capacity of HBC prepared by *in situ* fermentation with different levels of HPMC. Values in each sample with different superscripts (a–d) are significantly different ($n = 6$, $p < 0.05$).

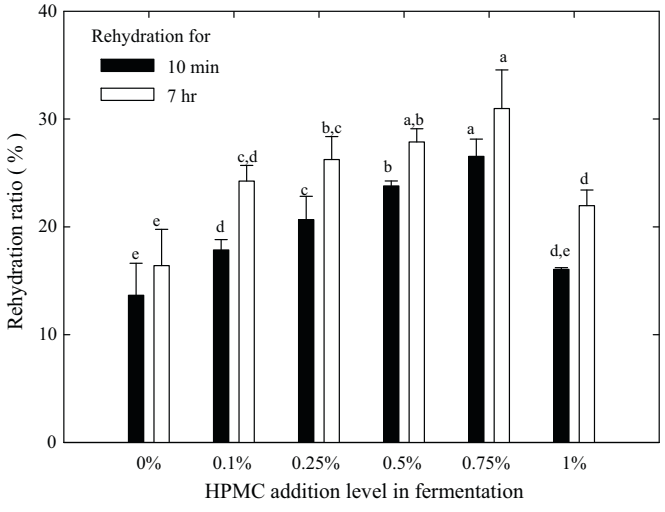

Fig. 6. Rehydration ratio of HBC prepared by *in situ* fermentation with different levels of HPMC. Values in each sample immersed for 10 min or 7 h with different superscripts (a–e) are significantly different ($n = 6$, $p < 0.05$).

Table 2
Hydrophilic properties and EMG absorption ability of BC and HBC.

Sample	Rehydration ratio (%)		EMG content (%)	Composition ratio
	10 min immersion	7 h immersion		
BC	13.65 ± 2.90[d]	16.40 ± 3.36[d]		
0.75%HBC	26.53 ± 1.60[c]	30.97 ± 3.59[c]		
BC/EMG	46.59 ± 0.54[b]	56.75 ± 3.30[b]	53.83 ± 2.55[b]	1.17 ± 0.05[b]
0.75%HBC/EMG	51.19 ± 2.42[a]	66.78 ± 2.93[a]	68.73 ± 2.89[a]	2.20 ± 0.07[a]

Values for each sample in a column with different superscripts (a–d) are significantly different ($n = 6$, $p < 0.05$).

In this study, WHC was determined under centrifugal force, and the relatively low WHC of HBC reflected the weaker water absorption ability of cellulose networks formed during *in situ* fermentation. Amorphous regions of BC increased as a result of the HPMC interfering with the H-bonds forming between microfibrils, which decreased the cystallinity and weakened the HPMC contained BC interpenetrating networks. Therefore, water molecules could not be absorbed well in the HBC during centrifuging. As HPMC addition levels increased to 1%, the crystallinity increased (Table 1) because the high concentration of HPMC could not be embedded between microfibrils. These free-type hydrophilic HPMCs were filled in the BC network and increased the degree of WHC in HBC. Notably, voids in such HBC networks were diminished, reducing the space to accommodate water molecules, which resulted in the rehydration ratio decrease.

3.6. Composition of HBC and EMG

The 0.75%HBC was selected to evaluate the low molecular compounds absorption ability since it possesses low crystallinity and high rehydration properties. EMG contents were 68.73% and 53.83% while the composition ratios were 2.20 and 1.17, in 0.75%HBC/EMG and BC/EMG, respectively (Table 2). The 0.75%HBC exhibited superior low molecular compound absorption ability to BC. Furthermore, rehydration ratio of the freeze dried 0.75%HBC/EMG came to 51.19% and 66.78% for 10 min and 7 h immersion, respectively. Such rehydration ability was higher than that of BC/EMG and was around 3-fold of BC and 2-fold of HBC. This revealed that the EMG significantly enhanced the rehydration of composites. Therefore, the hydrophilic property of EMG and lower crystallinity of its composite (Lin et al., 2009) were suggested to contribute to the rehydration ability.

4. Conclusion

The lower moduli, broader cellulose bundles width, and lower crystallinity of the HBC were observed as HPMC addition levels increased in fermentation. The interference of inter- and intra-microfibril textured mechanisms and the reduction in degree of crystallinity of nanoscale cellulose networks resulted in increased HBC rehydration capability. Notably, significant improvement in rehydration ability and small molecule absorption ability was obtained in 0.75%HBC. The nanocomposites, prepared from BC modified with HPMC and EMG, help overcome the rehydration limitations of dried BC while extending the storage time and possible applications of BC in bio-film systems.

Acknowledgements

The author wishes to thank the National Science Council (NSC 97-2313-B-197-011-MY3) for financial support of this study, and also express appreciation for the assistance of Huang, H.C. and Hsu, C.P. in the experiments.

References

Bodhibukkana, C., Srichana, T., Kaewnopparat, S., Tangthong, N., Bouking, P., Martin, G. P., et al. (2006). Composite membrane of bacterially-derived cellulose and molecularly imprinted polymer for use as a transdermal enantioselective controlled-release system of racemic propranolol. *Journal of Controlled Release*, *113*, 43–56.

Cannon, R. E., & Anderson, S. M. (1991). Biogenesis of bacterial cellulose. *Critical Reviews in Microbiology*, *17*, 435–447.

Clasen, C., Sultanova, B., Wilhelms, T., Heisig, P., & Kulicke, W.-M. (2006). Effects of different drying processes on the material properties of bacterial cellulose membranes. *Macromolecular Symposia*, *244*, 48–58.

Embuscado, M. E., BeMiller, J. N., & Marks, J. S. (1996). Isolation and partial characterization of cellulose produced by *Acetobacter xylinum*. *Food Hydrocolloids*, *10*, 73–82.

Engelhardt, J. (1995). Sources, industrial derivatives, and commercial applications of cellulose. *Carbohydrate in Europe*, *12*, 5–14.

Fengel, D., & Ludwig, M. (1991). Möglichkeiten und Grenzen der FTIR-Spektroskopie bei der charakterisierung von cellulose. *Das Papier*, *45*, 45–51.

Grande, C. J., Torres, F. G., Gomez, C. M., & Bano, M. C. (2009). Nanocomposites of bacterial cellulose/hydroxyapatite for biomedical applications. *Acta Biomaterialia*, *5*, 1605–1615.

Haigler, C. H., White, A. R., Brown, R. M., & Cooper, K. M. (1982). Alteration of in vivo cellulose ribbon assembly by carboxymethylcellulose and other cellulose derivatives. *Journal of Cell Biology*, *94*, 64–69.

Hirai, A., Tsuji, M., Yamamoto, H., & Horii, F. (1998). In situ crystallization of bacterial cellulose. III. Influences of different polymeric additives on the formation of microfibrils as revealed by transmission electron microscopy. *Cellulose*, *5*, 201–213.

Hong, L., Wang, Y. L., Jia, S. R., Huang, Y., Gao, C., & Wan, Y. Z. (2006). Hydroxyapatite/bacterial cellulose composites synthesized via a biomimetic route. *Materials Letters*, *60*, 1710–1713.

Intarasirisawata, R., Benjakul, S., Visessanguanb, W., Prodpranc, T., Tanaka, M., & Howell, N. K. (2007). Autolysis study of bigeye snapper (*Priacanthus macracanthus*) skin and its effect on gelatin. *Food Hydrocolloids*, *21*, 537–544.

Ivanova, N. V., Korolenko, E. A., Korolik, E. V., & Zbankov, R. G. (1989). Mathematical processing of IR-spectra of cellulose. *Zurnal Prikladnoj Spektroskopii*, *51*, 301–306.

Jonas, R., & Farah, L. F. (1998). Production and application of microbial cellulose. *Polymer Degradation and Stability*, *59*, 101–106.

Klemm, D., Schumann, D., Kramer, F., Hesler, N., Hornung, M., Schmauder, H.-P., et al. (2006). Nanocelluloses as innovative polymers in research and application. In D. Klemm (Ed.), *Polymer science, polysaccharides II* (pp. 49–96). Berlin, Heidelberg, Germany: Springer.

Koyama, M., Helbert, W., Imai, T., Sugiyama, J., & Henrissat, B. (1997). Parallel-up structure evidences the molecular directionality during biosynthesis of bacterial cellulose. *Biophysics*, *94*, 9091–9095.

Kramer, F., Klemm, D., Schumann, D., Heßler, N., Wesarg, F., Fried, W., et al. (2006). Nanocellulose polymer composites as innovative pool for (bio)material development. *Macromolecular Symposia*, *244*, 136–148.

Lin, S. B., Hsu, C. P., Chen, L. C., & Chen, H. H. (2009). Adding enzymatically modified gelatin to enhance the rehydration abilities of bacterial cellulose. *Food Hydrocolloids*, *23*, 2195–2203.

Maréchal, Y., & Chanzy, H. (2000). The hydrogen bond network in Iβ cellulose as observed by infrared spectrometry. *Journal of Molecular Structure*, *523*, 183–196.

Morris, E. R., & Ross-Murphy, S. B. (1981). Chain flexibility of polysaccharides and glycoproteins from viscosity measurement. In D. H. Northcote (Ed.), *Techniques in carbohydrate metabolism* (pp. 1–46). Amsterdam: Elsevier/North-Holland.

Musampa, R. M., Alves, M. M., & Maia, J. M. (2007). Phase separation, rheology and microstructure of pea protein-kappa-carrageenan mixtures. *Food Hydrocolloids*, *21*, 92–99.

Muyonga, J. H., Cole, C. G. B., & Duodu, K. G. (2004). Extraction and physico-chemical characterisation of Nile perch (*Lates niloticus*) skin and bone gelatin. *Food Hydrocolloids*, *18*, 581–592.

Nakayama, A., Kakugo, A., Gong, J. P., Osada, Y., Takai, M., Erata, T., et al. (2004). High mechanical strength double-network hydrogel with bacterial cellulose. *Advanced Functional Materials*, *14*, 1124–1128.

Nishi, Y., Uryu, M., Yamanaka, S., Watanabe, K., Kitamura, N., Iguchi, M., et al. (1990). The structure and mechanical properties of sheets prepared from bacterial cellulose. Part 2. Improvement of the mechanical properties of sheets and their applicability to diaphragms of electroacoustic transducers. *Journal of Materials Science*, *25*, 2997–3001.

Oh, S. Y., Yoo, D. I., Shin, Y., Kim, H. C., Kim, H. Y., Chung, Y. S., et al. (2005). Crystalline structure analysis of cellulose treated with sodium hydroxide and carbon dioxide by means of X-ray diffraction and FTIR spectroscopy. *Carbohydrate Polymers*, *340*, 2376–2391.

Okiyama, A., Motoki, M., & Yamanaka, S. (1992). Bacterial cellulose. II. Processing of the gelatinous cellulose for food materials. *Food Hydrocolloids*, *6*, 479–487.

Okiyama, A., Motoki, M., & Yamanaka, S. (1993). Bacterial cellulose. IV. Application to processed foods. *Food Hydrocolloids*, *6*, 503–511.

Reddy, G. K., & Enwemeka, S. (1996). A simplified method for the analysis of hydroxyproline in biological tissues. *Clinical Biochemistry*, *29*, 225–229.

Schwanninger, M., Rodrigues, J. C., Pereira, H., & Hinterstoisser, B. (2004). Effects of short-time vibratory ball milling on the shape of FT-IR spectra of wood and cellulose. *Vibrational Spectroscopy*, *36*, 23–40.

Segal, L., Creely, J. J., Martin, A. E. J., & Conrad, C. M. (1959). An empirical method for estimating the degree of crystallinity of native cellulose using the X-ray diffractometer. *Textile Research Journal*, *29*, 786–794.

Shimada, A., Yamamoto, I., & Sase, H. (1984). Surface properties of enzymatically modified proteins in aqueous system. *Agricultural and Biological Chemistry*, *48*, 2681–2688.

Šturcová, A., His, I., Apperley, D. C., Sugiyama, J., & Jarvis, M. C. (2004). Structural details of crystalline cellulose from higher plants. *Biomacromolecules*, *5*, 1333–1339.

Tokoh, C., Takabe, K., Sugiyama, J., & Fujita, M. (2002). CP/MAS 13C NMR and electron diffraction study of bacterial cellulose structure affected by cell wall polysaccharides. *Cellulose*, *9*, 351–360.

Uhlin, K. I., Atalla, R. H., & Thompson, N. S. (1995). Influence of hemicelluloses on the aggregation patterns of bacterial cellulose. *Cellulose*, *2*, 129–144.

Whitney, S. E. C., Brigham, J. E., Darke, A. H., Reid, J. S. G., & Gidley, M. J. (1995). In-vitro assembly of cellulose/xyloglucan networks – ultrastructural and molecular aspects. *The Plant Journal*, *8*, 491–504.

Yamada, Y., Hoshino, K., & Ishikawa, T. (1997). The phylogeny of acetic acid bacteria based on the partial sequences of 16S ribosomal RNA: the elevation of subgenus *Gluconacetobacter* to the generic level. *Bioscience, Biotechnology, and Biochemistry*, *61*, 1244–1251.

Yamada, Y., Hoshino, K., & Ishikawa, T. (1998). Gluconoacetobacter [sic], validation of publication of new names and new combinations previously effectively published outside the IJSB list No. 64. *International Journal of Systematic Bacteriology*, *48*, 327–328.

Yamamoto, H., Horii, F., & Hirai, A. (1996). In-situ crystallization of bacterial cellulose II. Influences of polymeric additives with different molecular weights on the formation of celluloses Iα and Iβ at the early stage of incubation. *Cellulose*, *3*, 229–242.

Yamamoto, I., Kusuhara, K., & Matsumoto, M. (1984). Phase behavior of enzymatically modified proteins in concentrated aqueous system. *Agricultural and Biological Chemistry*, *48*, 2689–2713.

Yamanaka, S., Watanabe, K., Kitamura, N., Iguchi, M., Mitsuhashi, S., Nishi, Y., et al. (1989). The structure and mechanical properties of sheets prepared from bacterial cellulose. *Journal of Materials Science*, *24*, 3141–3145.

Zugenmaier, P. (2001). Conformation and packing of various crystalline cellulose fibers. *Progress in Polymer Science*, *26*, 1341–1417.